Chiral Nanocrystals

DOI: 10.1002/anie.201207489

Enantioselective Synthesis of Intrinsically Chiral Mercury Sulfide Nanocrystals**

*Assaf Ben-Moshe, Alexander O. Govorov, and Gil Markovich**

Chirality is a key aspect in the evolution of life and plays an important role in structure–function relationships and recognition in biological systems. Interest in this property extends from fundamental particle physics and optics through organic and inorganic chemistry to complex biological systems, such as proteins and nucleic acids. The two mirror images of a chiral molecule (enantiomers) differ in their interaction with polarized light, and this difference gives rise to chiroptical activity. One of the commonly observed effects in such molecules is the differential absorption of left and right circularly polarized light, termed circular dichroism (CD).[1] Because of the connection between the chirality of molecules and their chemical function, a great amount of research has been carried out in the field of organic and inorganic chemistry with respect to control over chirality (enantioselective chemistry). Chiral symmetry breaking in the crystallization of various organic and inorganic materials[2–4] and various chiral amplification[5,6] templates are also of vast scientific interest owing to their relevance to the origin of homochirality in organisms.[7] In this respect, there is major interest in the crystallization of chiral inorganic minerals, such as quartz, and their role in enantioselective catalysis.[7,8]

Whereas mesoscale and nanoscale homochiral adsorption and self-assembly patterns of molecules have been produced on specific chiral surfaces,[9] so far there are no methods for the enantioselective synthesis of inorganic nanocrystals (NCs). NCs of intrinsically chiral materials should possess very strong chiroptical responses owing to their relatively large size relative to that of molecules, as long as they are of subwavelength dimensions. All recent studies on chirality in NCs has focused on controlling the assembly of achiral building blocks into chiral superstructures or generating typically weak chiroptical effects through the interaction chiral molecules with achiral metal and semiconductor NCs.

A relatively new field linking the properties of chirality and chiroptical activity with inorganic NCs has emerged with the first demonstration by Schaaff and Whetten of the induction of chiroptical activity in gold clusters capped with l-glutathione,[10] whereby CD was measured at electronic transitions of the inorganic gold core. Many studies on hybrid systems of chiral molecules and metal nanoparticles followed.[11–14] Later, following an initial demonstration by Gun'ko and co-workers,[15] studies were extended to semiconductor NCs of CdS,[16,17] CdSe,[18] and CdTe[19,20] capped with chiral molecules. It was assumed that the chiroptical effects arise mostly as a result of several mechanisms that involve some sort of CD induction by the capping chiral molecules. The first is the chiral distortion of surface atoms or the chiral adsorption pattern of the capping molecules on the surface of NCs.[21,22] In a recent study by Bürgi and co-workers,[23] it was demonstrated that the latter can result in relatively strong chiroptical activity in gold clusters. They demonstrated the postsynthesis enantiomeric separation of chiral inorganic clusters, similar to the enantiomeric separation of chiral macromolecules.

In the second CD-induction mechanism, the surface structure and the core are achiral, and chiroptical activity originates in electronic interactions ("dissymmetric field") between the capping molecules and the inorganic core.[10,24–26] This activity can arise, for example, by a simple dipolar interaction mechanism proposed and demonstrated experimentally by Govorov and co-workers.[27,28] It was also suggested for chiral-thiolate-protected gold clusters that the electronic contributions and geometric contributions might act concurrently.[29] Another possible origin of chiroptical effects is in strong coupling between achiral plasmonic NCs arranged in a chiral superstructure. Recent examples include the studies of Liedl and co-workers on metal nanoparticles assembled into chiral helices in DNA templates[30] and the studies of Liz-Marzán and co-workers on gold-nanorod assemblies.[31] Other than in the case of small atomic clusters, in which the core and surface are hard to differentiate, it has been assumed that chiroptical effects do not arise from the intrinsic chirality of the inorganic core, owing to the achiral symmetry of the crystal lattices of all materials studied so far. An exception was a study of microcrystals of trigonal (chiral) selenium in a cellulose matrix; these microcrystals exhibited CD at the absorption lines of the Se atoms.[32] Only one type of handedness of the crystals could be generated, and light-scattering effects, which may have been pronounced at the microscale, were not addressed. The magnitude of the CD signal observed in that study was relatively small, possibly because the nature of the electronic excitations in Se atoms. To the best of our knowledge, there have been no other

[*] A. Ben-Moshe, Prof. G. Markovich
School of Chemistry, Raymond and Beverly Sackler Faculty of Exact Sciences, Tel Aviv University
Tel Aviv, 69978 (Israel)
E-mail: gilmar@post.tau.ac.il
Prof. A. O. Govorov
Department of Physics and Astronomy, Ohio University
Athens, OH 45701 (USA)

[**] The help of Dr. Yuri Rosenberg with XRD measurements is gratefully acknowledged. This research was supported by the Israel Science Foundation (grant no. 172/10), the James Frank Program on light–matter interaction, and the NSF (USA). A.B.-M. is grateful to Marcel Adams and the Israel Academy of Science and Humanities for an Adams Fellowship.

Supporting information for this article is available on the WWW under http://dx.doi.org/10.1002/anie.201207489.

studies of micro- or nanoscale inorganic crystals of intrinsically chiral materials.

Herein we report the synthesis of α-HgS NCs, which belong to a chiral symmetry group, with a large enantiomeric excess. The synthesis makes use of chiral surfactant molecules (penicillamine), which direct the formation of these chiral NCs from the achiral phase of mercury sulfide (β-HgS). The strong chiroptical response of the obtained α-HgS NCs, which was several orders of magnitude larger than the CD response of achiral semiconductor NCs (CdS, CdSe, CdTe, ZnSe) coated with the same (or similar) chiral surfactant molecules, led to the conclusion that the α-HgS NCs were formed with high enantiomeric excess.

A variety of inorganic crystals, such as quartz, β-AgSe, α-HgS, selenium, and tellurium, are known to have intrinsically chiral crystal structures and have even occasionally been explored for their chiroptical properties in the form of bulk single crystals.[33,34] We suggest that NCs of materials of this type should exhibit much stronger chiroptical activity than previously reported for nanoparticle systems, in particular near wavelengths of spatially extended electronic transitions. The main idea was to use colloidal chemistry in an environment of a relatively large concentration of chiral molecules that could bind strongly to the surface of the forming crystals and induce symmetry breaking in the process. For this study, α-HgS (cinnabar) was chosen as a natural extension from type II–VI semiconductor materials previously studied,[16–21,26,35] with the advantage that α-HgS exhibits visible absorption lines (bulk band gap ≈ 2 eV) far away from the molecular UV absorption to enable the comfortable measurement of inorganic-core CD spectra.

HgS NCs were synthesized by a simple colloidal precipitation reaction in the presence of chiral molecules with thiolate groups, which were expected to bind strongly to Hg ions in the forming crystal (specifically, the molecule penicillamine was used; see the Experimental Section for details). The addition of S^{2-} ions to an aqueous solution of Hg^{2+} ions and penicillamine molecules was accompanied by the immediate appearance of a strong black color corresponding to achiral β-HgS NCs with a cubic zincblende structure. These NCs did not exhibit any CD in the visible range. The solution color gradually changed from black to orange in a matter of a few hours. The gradual change of color indicates that the achiral β phase was transformed into the thermodynamically favorable α phase. The stages of the transformation were monitored by transmission electron microscopy (TEM) and visible CD (see the Supporting Information). TEM images of the final orange-colored product showed the single-crystalline structure of these NCs (Figure 1). Image analysis indicated that the NCs had an average length of (15 ± 4) nm and an average width of (10 ± 3) nm.

The α-HgS phase was verified by powder XRD measurements, which are presented in Figure 1c with reference literature XRD data for bulk cinnabar.[36] In the α-HgS phase, the NCs exhibited a very strong CD band that was in good correlation with the band-edge absorption feature (Figure 2a,b). The dissymmetry factor ($\Delta\varepsilon/\varepsilon = \Delta A/A$) is a measure of the strength of the CD relative to the total absorption and normalizes out concentration dependence. In

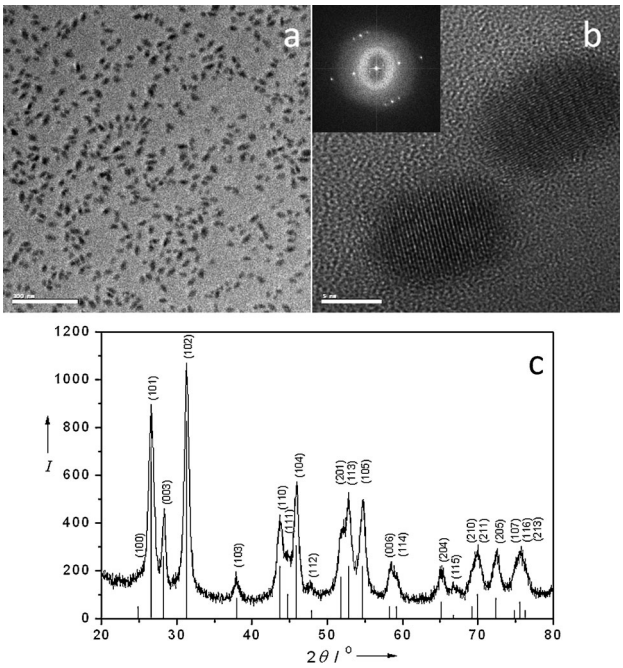

Figure 1. a) TEM image of HgS NCs. Scale bar is 100 nm. b) A high-resolution TEM image with the corresponding Fourier transform depicting the single-crystalline nature of these NCs. Scale bar is 5 nm. c) Powder XRD spectrum of this sample, presented with a reference bulk-phase diffraction pattern as thin vertical lines (Ref. [36]).

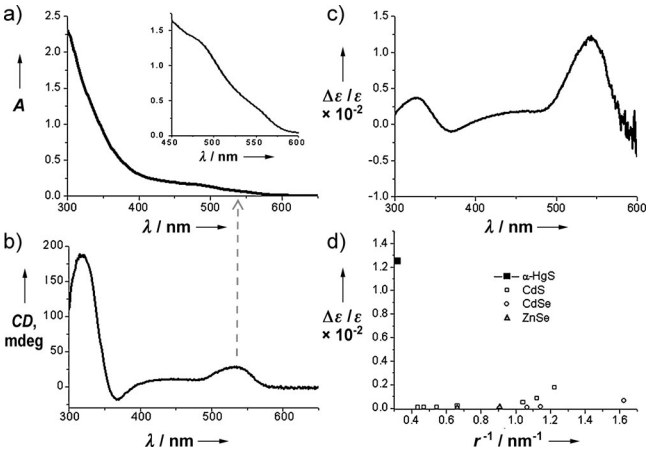

Figure 2. a) Absorption spectrum of the HgS NCs with the threshold range of 450–600 nm magnified for clarity in the inset. b) Corresponding CD spectrum; the dashed arrow marks the correlation between the first CD line and the absorption threshold. c) Corresponding dissymmetry spectrum. d) Dissymmetry factor at the first absorption/CD peak of various samples of NCs of different materials and sizes as a function of surface-to-volume ratio ($1/r$; r = NC radius).

the case of the α-HgS NCs, the dissymmetry values were over 0.012 for the first band-edge peak position and significantly larger than 0.001 throughout the rest of the spectrum (Figure 2c).

For comparison with the HgS NCs, we studied L-glutathione-capped ZnSe NCs as another type of type II–VI semiconductor NCs. These ZnSe NCs belong to an achiral

crystal-symmetry group (see the Supporting Information). The dissymmetry values for ZnSe in our study and other compounds investigated in previous studies[26,35] were found to decrease rapidly as the size of the NCs increased. This decrease in the dissymmetry values is due to the decay of the electronic CD induction at the electron–hole transitions by the chiral capping molecules. In fact, in CdS, CdSe, and ZnSe NCs, the ligand-induced CD completely vanishes for NCs of sizes over 3–4 nm, and at the smallest sizes, the dissymmetry factor is less than 0.001 (Figure 2d).

Thus, it is clear that the α-HgS NCs with sizes over 10 nm are completely off the scale with respect to all other studied semiconductor quantum dots in which the CD was induced by chiral surface molecules. Indeed, we can expect that the "bulk" chirality of an NC can be stronger than that induced by surface molecules, since the bulk CD effect is derived from all atoms in an NC, whereas the other effect originates only from a thin surface layer of atoms. Dissymmetry values of the order of 10^{-2} were so far only found in metal NCs assembled in chiral configurations with very strong interparticle plasmonic coupling.[30,31] For individual NCs, the present dissymmetry values are the highest values reported to date by a significant margin.

The XRD pattern obtained for the NCs is identical to the bulk crystal structure of cinnabar. This material crystallizes in two different enantiomorphic space groups, $P3_121$ and $P3_221$, which correspond to mirror images of the crystal. The two space groups exhibit exactly the same diffraction pattern and cannot be distinguished without chiroptical spectroscopy. The crystal is comprised of long helices of alternating mercury and sulfur atoms that spiral around the *c* axis of the hexagonal unit cell.[37] Bonds between adjacent atoms within the helix are much stronger than those formed between adjacent helices, which probably accounts for the elongation observed along the *c* axis of the NCs in high-resolution TEM images of single NCs (Figure 3a,b). The Fourier transform of the images (Figure 3a,b) shows that the long axis of the crystal is perpendicular to the (003) plane of the crystal and thus indicates that it is the *c* axis. The long axis of the NC correlated well with the *c* axis for all the NCs studied by TEM at high resolution. Figure 3c depicts single helices of opposite chirality, with one section enlarged inside the frame of the hexagonal unit cell. As all of the NCs appear to be single crystals, it is clear that each of them has to have a well-defined uniform handedness.

The use of opposite enantiomers of the capping chiral molecule penicillamine led to the formation of opposite enantiomers of the NCs, as indicated by the CD spectra (Figure 4). No apparent change in absorption was observed between the two samples. A mixture of both enantiomers resulted in a CD signal with an amplitude proportional to the molar excess of one enantiomer. This result probably indicates that both enantiomorphic NCs were formed statistically, whereby one enantiomer was formed in excess with respect to the other in proportion to the amounts of the two ligands present. The shape and size of the NCs did not depend on the ligand ratio.

Several considerations lead to the conclusion that the strong chiroptical activity stems from the formation of a large

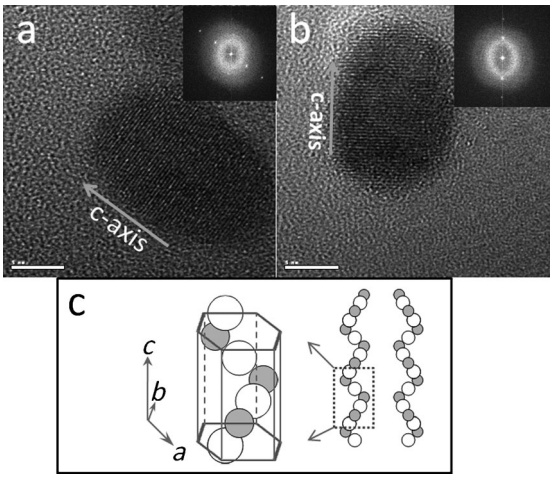

Figure 3. a,b) High-resolution TEM images of individual NCs; blue arrows mark the *c*-axis direction of the NC. Scale bars are 5 nm. In (a), a sketch of a single Hg–S helix (not to scale) has been placed on the image to correlate the direction of the Hg–S spirals with the crystal *c* axis. c) Schematic illustration of the opposite spirals of atoms with a fraction of one spiral reconstructed inside the frame of the hexagonal unit cell (based on the data from Ref. [36]).

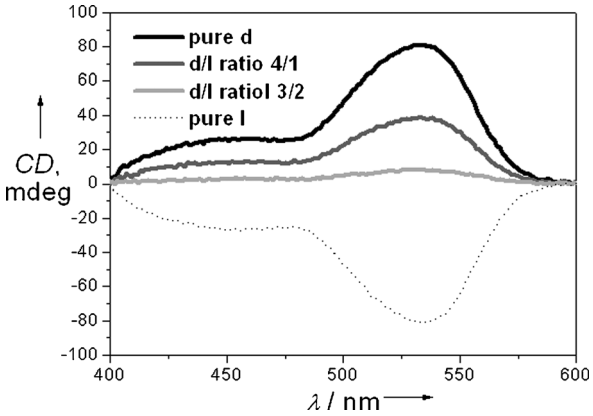

Figure 4. CD spectra of samples obtained at different molar ratios of L- and D-penicillamine with the same total concentrations of Hg and penicillamine. The use of 100% of one enantiomer resulted in the strongest CD response: the L and D enantiomers promoted the formation of opposite mirror images of the NCs. Mixed compositions of L- and D-penicillamine resulted in samples with a CD response that was proportional to the excess amount of one enantiomer in solution. The absorption spectra of all samples were identical.

enantiomeric excess of one of the enantiomorphs of cinnabar NCs. The strength of the effect in comparison with that of other semiconductors with achiral crystal structures excludes an electronic induction mechanism as well as surface-distortion effects. The larger size of the α-HgS NCs relative to that of semiconductor and metal clusters previously studied in the field of chiroptically active NCs also excludes a surface-related mechanism, since the surface-to-volume ratio is much smaller in the α-HgS NCs than in previously studied NCs and in the ZnSe NCs in the present study. Third, the crystal phase has been proven to be the intrinsically chiral phase of HgS. All these findings lead us to conclude that the mechanism for the

observed immensely strong chiroptical activity is directly related to the crystal core, and that the large excess of one enantiomer in solution is enabled by the chemistry developed in this study.

A simple theory of a chiral NC can be developed on the basis of the continuous-medium approach by using the local properties of a crystal, such as a local dielectric function $\varepsilon(r)$ and a local chiral parameter $\xi(r)$. This approach, which ignores the spatial quantitation of carriers, is justified for our relatively large NCs. A convenient, analytically solvable model presented by Govorov and Fan is a chiral absorbing sphere.[38] The CD cross-section of such a physical object has two terms: CD_{ξ}, the CD due to the intrinsic chirality of the NC as screened dynamically in terms of the dielectric response of the NC, and CD_{ε}, the CD due to the near-field interaction between the absorptive and chiral properties of an object (for details, see the Supporting Information):

$$\begin{aligned} CD_{\xi} &= AR_{NC}^{3}\,\mathrm{Im}[\xi_{NC}]\,\frac{\mathrm{Re}[2\varepsilon_0+\varepsilon_{NC}]}{|2\varepsilon_0+\varepsilon_{NC}|^2}, \\ CD_{\varepsilon} &= -AR_{NC}^{3}\,\frac{\mathrm{Re}[\xi_{NC}]\mathrm{Im}[\varepsilon_{NC}]}{|2\varepsilon_0+\varepsilon_{NC}|^2} \end{aligned} \tag{1}$$

In Equation (1), the parameter ε_{NC} is the dielectric function of the HgS NCs, ξ_{NC} is a parameter describing the intrinsic chiral response of the HgS crystal, $\varepsilon_0 = \varepsilon_{water}$, and R_{NC} is the NC radius. The second mechanism [i.e. the CD_{ε} term in Eq. (1)] is relatively weak for the HgS NC, but it was found to be very important for metal NCs conjugated with chiral biomolecules.[27,28] To the best of our knowledge, the CD of bulk HgS has not been reported so far. In this study, we had the chance to estimate this property of α-HgS by comparing the simple theory [Eq. (1)] with the experiment on HgS NCs. Our analysis (see the Supporting Information) led to the following values for the molar CD per HgS molecule, the chiral parameter ξ_{HgS}, and the specific rotation of HgS: $\Delta\varepsilon_{CD,molecule} \approx 0.61\,M^{-1}cm^{-1}$ (535 nm); ξ_{HgS}: $(0.61+3.6i)\times10^{-4}$; $\alpha_{deg} \approx 125\,deg\,mm^{-1}$. These values are physically reasonable and comparable with the parameters of some other chiral crystals and materials (see the Supporting Information). The earlier measurement[39] and theoretical treatment[40] of the optical rotation of bulk HgS yielded values of specific rotation which are slightly higher (by a factor of 3–5) than those calculated by us for the red edge of the spectrum at 600–650 nm. In contrast to the present case, bulk measurements could not be extended beyond the absorption threshold to higher energies owing to total absorption of the incident light. The difference in specific rotation between the bulk material and nanocrystals is expected for two reasons. First, the local crystal parameters of a relatively small NC (ε_{NC} and ξ_{NC}) can be somewhat different to those in the bulk because of the surface effects. A second pronounced effect is the orientation of the crystal relative to the light-propagation direction. The bulk measurements were executed on single crystals oriented with the *c* axis of the crystal parallel to the light-propagation direction. Since HgS is optically highly anisotropic and in the study presented herein the sample consists of randomly oriented NCs, only a fraction of the nanocrystals would be oriented parallel to the light-wave vector. Consequently, averaging over the different orientations in the colloidal NC sample would result in weaker effects.

In summary, a new concept of enantioselective chemistry of inorganic NCs on the basis of chiral crystal symmetry groups is proposed, with a first proof of concept for α-HgS NCs. This approach is very different from previous ideas on the induction of chiroptical activity in achiral NCs and will probably lead to very intriguing effects in a wide range of materials. The generation of truly chiral NCs of tailored size and shape is expected to be useful for many applications, such as enantioselective catalysis and sensing. Furthermore, these systems are intriguing for studies in more fundamental fields, such as nanoscale photophysics and electronic theory, as a result of the combination of chirality with quantum confinement effects. It is expected that this concept should be applicable to the enantioselective synthesis of nanostructures of other chiral inorganic crystals.

Experimental Section

Synthesis of HgS NCs: An aqueous solution of $Hg(NO_3)_2$ (100 mM, 0.9 mL) was added to water (3 mL), and then an aqueous solution of penicillamine (0.9 mL) with a particular enantiomeric composition (total concentration of the two enantiomers: 100 mM) was added. The resulting mixture was stirred vigorously, and its pH value was increased slowly to approximately 11.5 by the addition of aqueous NaOH. An aqueous thioacetamide solution (100 mM, 0.9 mL) was then quickly added, whereupon the solution immediately turned black. The reaction mixture was stirred in the dark at room temperature for 24 h. Isopropyl alcohol was then added to precipitate the product from the solution. The resulting orange-colored HgS NCs were collected after centrifugation, washed several times with a 9:1 isopropanol–water mixture, and finally redispersed in water.

Detailed procedures for the synthesis of CdS and CdSe samples corresponding to the data in Figure 2d appear in Ref. [35], and details of the synthesis of glutathione-coated ZnSe NCs appear in the Supporting Information.

TEM images were recorded with an FEI Tecnai F20 FEG-TEM instrument. All samples were placed on carbon-coated 300-mesh Cu grids. X-ray diffraction data was collected with $Cu_{K\alpha}$ radiation on a Θ-Θ Scintag powder diffractometer equipped with a Ge solid-state detector cooled with liquid nitrogen. CD measurements were performed on an Applied Photophysics Chirascan CD spectrometer. Absorption measurements were performed on a Varian Carry 5000 spectrophotometer. Samples were diluted with water to concentrations at which the absorbance value was around 0.1 at about 500 nm.

Received: September 16, 2012
Revised: November 7, 2012
Published online: December 11, 2012

Keywords: chiral resolution · chirality · circular dichroism · inorganic nanocrystals · nanoparticles

[1] *Circular Dichroism: Principles and Applications* (Eds.: K. Nakanishi, N. Berova, R. W. Woody), Wiley-VCH, New York, **2000**.
[2] D. K. Kondepudi, R. J. Kaufman, N. Singh, *Science* **1990**, *250*, 975–977.
[3] C. Viedma, *Phys. Rev. Lett.* **2005**, *94*, 065504.
[4] L. Addadi, Z. Berkovitch-Yellin, I. Weissbuch, J. Van Mil, L. J. W. Shimon, M. Lahav, L. Leiserowitz, *Angew. Chem.*

1985, *97*, 476 – 496; *Angew. Chem. Int. Ed. Engl.* **1985**, *24*, 466 – 485.
[5] K. Soai, T. Shibata, H. Morioka, K. Choji, *Nature* **1995**, *378*, 767 – 768.
[6] H. Zepik, E. Shavit, M. Tang, T. R. Jensen, K. Kjaer, G. BolBach, L. Leiserowitz, I. Weissbuch, M. Lahav, *Science* **2002**, *295*, 1266 – 1269.
[7] W. A. Bonner, *Origins Life Evol. Biosphere* **1991**, *21*, 59 – 111.
[8] K. Soai, S. Osanai, K. Kadowaki, S. Yonekubo, T. Shibata, I. Sato, *J. Am. Chem. Soc.* **1999**, *121*, 11235 – 11236.
[9] See, for example: S. Haq, N. Liu, V. Humblot, A. P. J. Jansen, R. Raval, *Nat. Chem.* **2009**, *1*, 409 – 414, and references therein.
[10] T. G. Schaaff, R. L. Whetten, *J. Phys. Chem. B* **2000**, *104*, 2630 – 2641.
[11] C. Gautier, T. Bürgi, *J. Am. Chem. Soc.* **2006**, *128*, 11079 – 11087.
[12] H. Yao, T. Fukui, K. Kimura, *J. Phys. Chem. C* **2007**, *111*, 14968 – 14976.
[13] C. Gautier, T. Bürgi, *ChemPhysChem* **2009**, *10*, 483 – 492.
[14] G. Shemer, O. Krichevski, G. Markovich, T. Molotsky, I. Lubitz, A. B. Kotlyar, *J. Am. Chem. Soc.* **2006**, *128*, 11006 – 11007.
[15] M. P. Moloney, Y. K. Gun'ko, J. M. Kelly, *Chem. Commun.* **2007**, 3900 – 3902.
[16] M. Naito, K. Iwahori, A. Miura, M. Yamane, I. Yamashita, *Angew. Chem.* **2010**, *122*, 7160 – 7163; *Angew. Chem. Int. Ed.* **2010**, *49*, 7006 – 7009.
[17] R. Zhou, K. Y. Wei, J. S. Zhao, Y. B. Jiang, *Chem. Commun.* **2011**, *47*, 6362 – 6364.
[18] S. A. Gallagher, M. P. Moloney, M. Wojdyla, S. J. Quinn, J. M. Kelly, Y. K. Gun'ko, *J. Mater. Chem.* **2010**, *20*, 8350 – 8355.
[19] Y. Zhou, M. Yang, K. Sun, Z. Tang, N. A. Kotov, *J. Am. Chem. Soc.* **2010**, *132*, 6006 – 6013.
[20] T. Nakashima, Y. Kobayashi, T. Kawai, *J. Am. Chem. Soc.* **2009**, *131*, 10342 – 10343.
[21] S. D. Elliott, M. P. Molonet, Y. K. Gun'ko, *Nano Lett.* **2008**, *8*, 2452 – 2457.
[22] P. D. Jadzinsky, G. Calero, C. J. Ackerson, D. A. Bushnell, R. D. Kornberg, *Science* **2007**, *318*, 430 – 433.
[23] I. Dolamic, S. Knoppe, A. Dass, T. Bürgi, *Nat. Commun.* **2012**, *3*, 798.
[24] H. Yao, K. Miki, N. Nishida, A. Sasaki, K. Kimura, *J. Am. Chem. Soc.* **2005**, *127*, 15536 – 15543.
[25] M. Zhu, H. Quian, X. Meng, S. Jin, Z. Wu, R. Jin, *Nano Lett.* **2011**, *11*, 3963 – 3969.
[26] Y. Zhou, Z. Zhu, W. Huang, W. Liu, S. Wu, X. Liu, Y. Gao, W. Zhang, Z. Tang, *Angew. Chem.* **2011**, *123*, 11862 – 11866; *Angew. Chem. Int. Ed.* **2011**, *50*, 11658 – 11661.
[27] A. O. Govorov, Z. Fan, P. Hernandez, J. M. Slocik, R. R. Naik, *Nano Lett.* **2010**, *10*, 1374 – 1382.
[28] J. M. Slocik, A. O. Govorov, R. R. Naik, *Nano Lett.* **2011**, *11*, 701 – 705.
[29] A. Sánchez-Castillo, C. Noguez, I. L. Garzón, *J. Am. Chem. Soc.* **2010**, *132*, 1504 – 1505.
[30] A. Kuzyk, R. Schreiber, Z. Fan, G. Pardatscher, E. M. Roller, A. Högele, F. C. Simmel, A. O. Govorov, T. Liedl, *Nature* **2012**, *483*, 311 – 314.
[31] A. Guerrero-Martínez, B. Auguié, J. L. Alonso-Gómez, S. Gómez-Graña, Z. Džolic, M. Žinic, M. M. Cid, L. M. Liz-Marzán, *Angew. Chem.* **2011**, *123*, 5613 – 5617; *Angew. Chem. Int. Ed.* **2011**, *50*, 5499 – 5503.
[32] F. D. Saeva, G. R. Olin, J. Y. C. Chu, *Mol. Cryst. Liq. Cryst.* **1977**, *41*, 5 – 9.
[33] A. R. Bungay, Y. P. Svirko, N. I. Zheludev, *Phys. Rev. Lett.* **1993**, *70*, 3039 – 3042.
[34] K. C. Nomura, *Phys. Rev. Lett.* **1960**, *5*, 500 – 501.
[35] A. Ben Moshe, D. Szwarcman, G. Markovich, *ACS Nano* **2011**, *5*, 9034 – 9043.
[36] Swanson et al., *Natl. Bur. Stand. Circ. (U. S.)* **1955**, *539*(IV), 17.
[37] K. L. Aurivillius, *Acta Chem. Scand.* **1950**, *4*, 1413 – 1436.
[38] A. O. Govorov, Z. Fan, *ChemPhysChem* **2012**, *13*, 2551.
[39] F. A. Molby, *Phys. Rev.* **1910**, *31*, 291 – 310.
[40] S. Chandrasekhar, *Proc. Math. Sci.* **1953**, *37*, 697 – 703.

